

## Effect of Graphene Quantum Dots on the Capacitance Performances of flexible PEDOT: PSS films

Wenqian Yao<sup>1, ‡</sup>, Liying Li<sup>1, ‡</sup>, Zhiru Bai<sup>1</sup>, Yu Jiang<sup>1</sup>, Linya Xu<sup>1</sup>, Jiaqi Yan<sup>1</sup>, Yan Wan<sup>1</sup>, Rongri Tan<sup>2,\*</sup>, Huixuan Liu<sup>2</sup>, Peipei Liu<sup>2,\*</sup>

<sup>1</sup> Jiangxi Key Laboratory of Organic Chemistry, Jiangxi Science and Technology Normal University, Nanchang 330013, P. R. China

<sup>2</sup> Department of Physics, Jiangxi Science and Technology Normal University, Nanchang 330013, P. R. China

<sup>‡</sup> These authors contributed equally.

\*E-mail: [rogertan@hotmail.com](mailto:rogertan@hotmail.com) (R. Tan) and [liupeipei8866@126.com](mailto:liupeipei8866@126.com) (P. Liu).

Received: 8 May 2020 / Accepted: 21 June 2020 / Published: 10 August 2020

Supercapacitors are promising energy storage and power output technologies that can be used for practical energy conversion and storage devices are still urgently needed. Here, we prepared a free-standing flexible PEDOT:PSS/GQDs composite films, which contains PEDOT:PSS and variable contents GQDs, by a facile vacuum filtration method. And then the capacitance performance of PEDOT:PSS/GQDs films were systematically investigated and compared with pure PEDOT:PSS by cyclic voltammetry (CV), galvanostatic charge/discharge, and electrochemical impedance spectroscopy (EIS) measurements. These results show that the capacitance performance of the PEDOT:PSS/GQDs composites film incorporating GQDs components is improved in the H<sub>2</sub>SO<sub>4</sub> (1 M) electrolyte system under applied potential window (-0.2-0.8 V) as shown in the following aspects. The as-prepared films show excellence redox performance and rate capability, and the specific capacitance of film calculated by the galvanostatic charge/discharge curves reaches the maximum 21.5 mF cm<sup>-2</sup> at 20 wt.% GQDs composition compared to the prepared pure PEDOT:PSS (17.5 mF cm<sup>-2</sup>). Moreover, it displays excellent capacitance retention well over 84% of the initial value over 13500 consecutive charging/discharging cycles in air atmosphere, suggesting that PEDOT:PSS/GQDs film based on PEDOT:PSS and GQDs components have improved capacitive performance through the addition of high performance GQDs, which will provide important reference value for novel supercapacitor electrode materials.

**Keyword:** PEDOT:PSS; GQDs; Supercapacitors; Composite film; Organic polymer

### 1. INTRODUCTION

Supercapacitors also called electrochemical capacitors, are significative devices for energy conversion and storage in the era of shortage of chemical energy resources.[1-4] Compared to

conventional rechargeable batteries, supercapacitors with high power density, fast charge-discharge rates and long cycle life and environmentally friendly advantages appear to be largely in line with the needs of modern consumers for new energy sources have developed rapidly.[5-7] Supercapacitors can serve as a major complement to traditional energy storage devices, or even substitute for them, in energy storage and harvesting application.[8] The types of supercapacitors are mainly divided into electrical double layer capacitors and pseudocapacitors according to their mechanism of charge storage, in the former, electrons exist in electrodes and electrolytes interface as double layers, while in the pseudocapacitors, the capacitance is derived from the transfer of electrons at the electrode and electrolyte through a faradaic reaction.[9] The electrode is very important in these two kinds of supercapacitors, which plays a decisive role in the charge–discharge process, which directly determines the specific capacitance, long cycle life, potential window of supercapacitors.[10] Therefore, the research of electrode materials in the field of supercapacitors is of great significance. Yet they are mainly facing some challenges e.g. with a lower operating voltage and a lower energy density.

The development of composites comprising organic conducting polymers (CPs) and nanostructured materials as supercapacitor electrodes has flourished in recent years.[11-15] Among these classical composites, the typical organic conducting polymer poly (3,4-ethylenedioxythiophene):poly(styrenesulfonate) (PEDOT:PSS) was always introduced to improve the performance of supercapacitors and good optimization results have been reported.[16-19] Take the following example, Su group fabricated a uniform  $\text{MnO}_2$ –PEDOT:PSS nanocomposite electrode with specific capacitance of  $503 \text{ F g}^{-1}$  at  $1 \text{ mV s}^{-1}$ , [20] and Cheng group prepared a flexible transparent PEDOT:PSS/Ag grids exhibited superior electrochemical energy storage behaviours.[21] The above results are largely attributed to the fact that PEDOT:PSS is a promising supercapacitor electrode as a charge storage material, mainly due to its high conductivity, good electrochemical stability, as well as the conjugated backbone, which can easily transport delocalized electrons through p orbital systems. However, as a typical organic polymer, PEDOT:PSS still face the problem of poor capacitive performance, which leads to the inability to be applied to practical supercapacitors as an energy storage and conversion devices. Nowadays, the researchers mainly studied in the form of PEDOT:PSS based nanostructured composites, such as containing carbon nanotubes (CNTs), [22] to further explore excellent supercapacitor electrode materials for energy storage.

Graphene quantum dots (GQDs), is one of the forms of carbon material, which are single or few layer graphene, represent a novel quantum dot (QDs) with only a few nanometers of tiny size, and thus have a larger specific area, more active sites on the surface and more accessible edges, which can conveniently provide sufficient interfaces for ion adsorption/desorption, which has attracted wide attention and long-term research.[23-25] GQDs have shown great application prospects in photovoltaic devices, bio-imaging devices, lithium ion batteries and other applications due to their unique properties. Up to now, GQDs has become more popular in the field of supercapacitor electrode materials by virtue of its high specific surface area, good electrical conductivity, and nanometer size and good dispersion in various solvents and has been active in the field of electronic materials. Researchers reported a number of results that could significantly improve the performance of supercapacitor electrode materials by introducing GQDs components. It is expounded that GQDs can provide an outstanding interface for the interactions between electrodes and electrolytes, improving capacitance performance.[26, 27]

Researchers have further investigated GQDs as electrode devices for supercapacitors with slightly worse rate capability than GQDs based composites. Liu group, for example, confirmed that the capacitive performance of GQDs/MnO<sub>2</sub> was higher than that of GQDs/GQDs as a typical symmetric microsupercapacitor due to the pseudo-capacitance contribution of the MnO<sub>2</sub>. [28] Besides, some relevant articles on the design/preparation of novel materials for GQD and their complexes have also been reported in supercapacitor materials, confirming that GQDs would be an ideal supercapacitor electrode material candidate owing to high specific surface area and edge effects, etc. Inspired by the above, we designed and prepared a novel PEDOT:PSS/GQDs composite film for the study of electrode properties of supercapacitors. Here it is expected that the successful preparation of this PEDOT:PSS/GQDs material with low cost and high quality performance will be of great significance in the research of supercapacitor electrode materials.

Herein, we introduce a simple and low-cost vacuum filtration method to prepare a series of PEDOT:PSS/GQDs films containing variable GQDs concentrations ranging from 5 to 20 wt.%. All systemic electrochemical behavior curves analysis shows that the introduction of GQDs components can obviously improve the capacitance performance of the films, and the composite film with optimal capacitive performance can be obtained at GQDs with a content of 20 wt.% including the maximum specific capacitance and ultra-long cycling stability. All the experimental results details are discussed as follows.

## 2. EXPERIMENTAL

### 2.1 Chemicals

Poly (3,4-ethylenedioxythiophene):poly(styrenesulfonate) (PEDOT:PSS) was purchased from Shanghai J&K Scientific Ltd without further purification before use. Dimethyl sulfoxide (DMSO), sulfuric acid and ethyl alcohol were all purchased from Shanghai J&K Scientific Ltd and these solvents have analytical grade purity without further treatment.

### 2.2 Preparation of GQDs.

GQDs can be prepared by simple chemically cleaving graphene oxide (GO) processes, the detailed steps are as follows. 0.100 g GO was added to 10.0 mL distilled water and disperse treatment via ultrasonic treatment. Then 200.0 mL H<sub>2</sub>O<sub>2</sub> (30%) and 50.0 mL ammonia (25-28%) solution were successively added to the uniformly dispersed GO solution, and the above solution was stirred at 90 °C for 24 hours. Finally, the rotary evaporation method was used to remove the residual solution, GQDs were obtained via washing with ethanol and drying at 60 °C.

### 2.3 Composite PEDOT:PSS/GQDs film

The preparation process of PEDOT: PSS/GQDs film is simple and low cost as shown in Fig. 1, and the specific steps are as follows. First, the 300μL of PEDOT:PSS, different mass ratios of GQDs (5

wt.%, 10 wt.%, 15 wt.%, 20 wt.%), and 21  $\mu\text{L}$  of DMSO were dissolved into ethyl alcohol to total volume of 6 mL, respectively, and stirred it to form a solution without precipitation. The solution was carefully transferred to the suction device for filtration. Then the film on the PVDF micro-filtration membrane can be easily transferred into the plastic sheet. Finally, the newly prepared PEDOT:PSS/GQDs film was dried in a vacuum atmosphere of 150 °C for 2 h for the next test.

#### 2.4 Test of electrochemical properties

All electrochemical experiments including cyclic voltammetry (CV), galvanostatic charge/discharge, and electrochemical impedance spectroscopy (EIS) were performed in a three-electrode cell controlled by a computer at room temperature. The experimental cell consisting of the prepared PEDOT:PSS/GQDs film as the working electrode, platinum sheet as the counter electrode, and Ag/AgCl electrode as the reference electrode placed in 1 M sulfuric acid aqueous electrolyte solution. It's worth noting that the PEDOT:PSS/GQDs film needs to be activated by immersing in sulfuric acid (1 M) for 1 hour before testing.



**Figure 1.** Schematics of the process for fabricating the PEDOT:PSS/GQDs film.

### 3. RESULTS AND DISCUSSION

#### 3.1 Capacitance performance

The supercapacitor performances of the as-prepared PEDOT:PSS and PEDOT:PSS/GQDs composite films were evaluated by means of cyclic voltammetry (CV), galvanostatic charge–discharge, electrochemical impedance spectroscopy (EIS) in a three-electrode cell controlled by a computer in electrolyte solution.[29, 30] The CVs measurements of PEDOT:PSS and PEDOT:PSS/GQDs

composites with varying GQDs concentrations were performed in the  $\text{H}_2\text{SO}_4$  (1 M) system as shown in Fig. 2 A. The CV curve of PEDOT:PSS exhibits a rectangular shape with considerably high capacity at a scan rate of  $50 \text{ mV}^{-1}$  in the potential range from  $-0.2$  to  $0.8 \text{ V}$ , indicating that the charge–discharge responses of the electric double layer are highly reversible and kinetically facile, which is consistent with the results reported before.[8, 31] Nevertheless, it is evident from the CV curves of PEDOT:PSS/GQDs composite at the same potential window that they all show not completely rectangular shapes accompanied by a pair of redox peaks as pseudocapacitance, which can be attributed to the fast and reversible faradic redox reactions occurring in the electroactive materials.[32] Compared with pure PEDOT:PSS, PEDOT:PSS/GQDs composites containing different mass ratios GQDs (5 wt.%, 10 wt.%, 15 wt.%, 20 wt.%) show larger capacitance, the area of each closed CV curve suggests its capacitance, which means that the PEDOT:PSS/GQDs composites film were successfully prepared and has better capacitance performance. Taking the CVs of 20% GQDs mixture as an example, it can be analyzed from the Fig. 2B that the shapes of these curves remain similar with the increase of scanning rate from  $5$ – $300 \text{ mV s}^{-1}$ , which means that the composite has good redox and electrochemical properties.

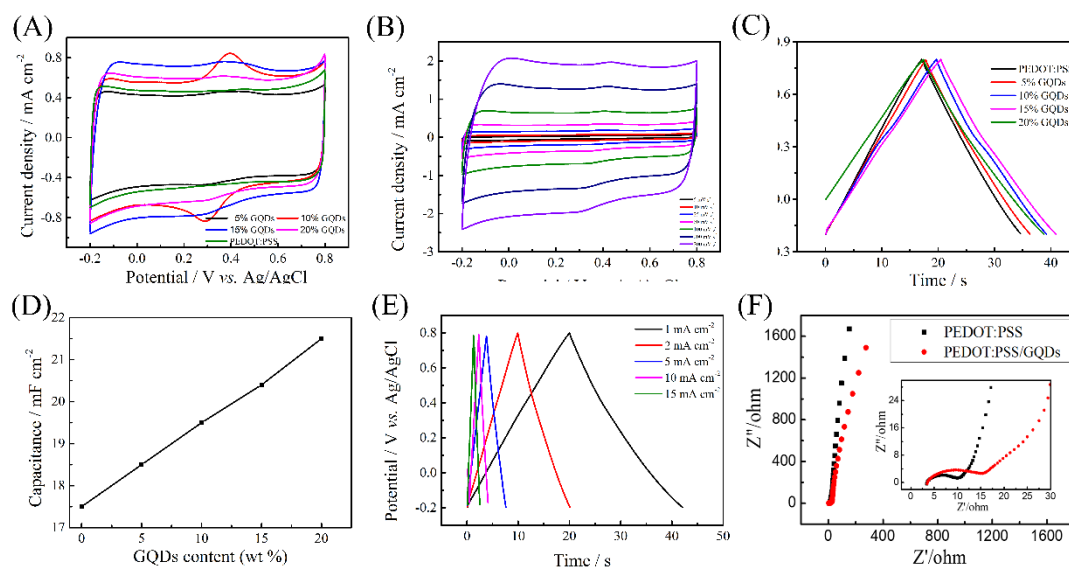


**Figure 2.** (A) CV curves of PEDOT:PSS and PEDOT:PSS/GQDs film with varying GQDs concentration recorded at  $50 \text{ mV s}^{-1}$ , (B) CV curves PEDOT:PSS/GQDs (20 wt %) at scan rates of  $5$ – $300 \text{ mV s}^{-1}$ , (C) galvanostatic charge/discharge curves of the PEDOT:PSS and PEDOT:PSS/GQDs composites film with varying GQDs concentrations taken at  $1 \text{ mA cm}^{-2}$  current density, (D) specific capacitance for PEDOT:PSS/GQDs composites film with varying GQDs concentrations calculated at  $1 \text{ mA cm}^{-2}$  current density, (E) galvanostatic charge/discharge curves of the PEDOT:PSS/GQDs (20 wt %) taken at different current densities and (F) Nyquist plot (with inset) for PEDOT:PSS/GQDs (20 wt %) film in 1 M  $\text{H}_2\text{SO}_4$  electrolyte system.

To gain deeper insights into the capacitive performances of the PEDOT:PSS/GQDs composites, a galvanostatic charge–discharge test was carried out here, as with PEDOT:PSS curve, all curves maintain a similar state of symmetry at a high current density of  $1 \text{ A g}^{-1}$ , which implies high reversibility between charge and discharge processes.

**Table 1.** Graphene, CNTs, PEDOT:PSS based composites used as supercapacitor electrode material

Composite	Method of preparation	Specific capacitance mF cm <sup>-2</sup>	Electrolyte	Reference
NFC/PEDOT-PSS	Screenprinting technique	8.5-9.5	1 M LiClO <sub>4</sub> /ACN	[33]
PEDOT/PSS-SWNT	Vacuum filtration	932	1 M NaNO <sub>3</sub>	[34]
rGO–PEDOT:PSS	Solution cast	535.4	1 M H <sub>2</sub> SO <sub>4</sub>	[35]
PEDOT:PSS/rGO/Eco	Porous-skeleton substrate	38.7	Aqueous	[31]
PEDOT:PSS	Spin coating	1.64	1 M H <sub>2</sub> SO <sub>4</sub>	[36]
CC/PEDOT:PSS-rGO	Spray technique	3000	PVA/H <sub>3</sub> PO <sub>4</sub>	[37]
Fe <sub>3</sub> O <sub>4</sub> @NG	Dry pyrolysis method	1480	6 M KOH	[38]
MnO <sub>2</sub> /graphene	One-pot approach	204.8	1M Na <sub>2</sub> SO <sub>4</sub>	[39]
PEDOT:PSS/GQDs	Vacuum filtration	21.5	1 M H <sub>2</sub> SO <sub>4</sub>	This work

The specific capacitance was calculated from galvanostatic charge–discharge curve using the current density, the formula is as follows,  $C_{s1} = I \times \Delta T_d / S \times \Delta V$ , where  $I$  and  $\Delta T_d$  represent the discharge current and the discharge time, respectively,  $\Delta V$  is discharge potential range, and  $S$  is the surface area of the electrode.[33] The specific capacitance of the varied compositions of GQDs–PEDOT:PSS/GQDs can be calculated using the formula mentioned above, that is 18.5 mF cm<sup>-2</sup> (5 wt.%), 19.5 mF cm<sup>-2</sup> (10 wt.%), 20.4 mF cm<sup>-2</sup> (15 wt.%), 21.5 mF cm<sup>-2</sup> (20 wt.%), respectively. As a result, the specific capacitance of reaching the maximum 21.5 mF cm<sup>-2</sup> at 20 wt.% GQDs composition of PEDOT:PSS/GQDs compared to the prepared pure PEDOT:PSS (17.5 mF cm<sup>-2</sup>) and the composites containing other different mass ratios GQDs, as shown in figure 2 D, indicating introduction of an appropriate concentration of GQDs, the amount of PEDOT:PSS/GQDs is ascertained in ideal state at 20 wt.% GQDs composition, which facilitates the formation of the composite with a larger specific surface area, and makes more interfacial surface between the nanostructures and the electrolyte, which leads to the increase of capacitance performance.[34] Therefore, it concluded that the supercapacitor electrodes based on PEDOT:PSS/GQDs film have high capacitance due to the combination of the excellent conducting and excellent capacitance performance of GQDs. Besides, we further study the capacitance behaviour of PEDOT:PSS/GQDs (20 wt.%) composite film at different current densities, it can be seen clearly that almost all curves are near triangle-shaped curves (Fig. 2E), the symmetry of the charge/discharge curves indicates the composite film has high reversibility, rate capability, and with the increase of applied current, the discharge time decreases significantly with the decrease of specific capacitance, which is a common phenomenon, which may be attributed to the film swelling as the electrolyte ions intercalate in and out of the film, as well as some energy loss to irreversible processes that lead to hysteresis.[35] Here, we make a tabular summary of these composites and make corresponding analysis to obtain a more comprehensive understanding of graphene, CNTs, PEDOT:PSS based composites used as supercapacitor electrode material in recent years, as shown in Table 1. Compared to pure PEDOT:PSS reported, the SWNT/rGO–PEDOT:PSS composites electrode materials based PEDOT:PSS and the

second treated PEDOT:PSS have significantly enhanced specific capacitance and it is concluded that the preparation of composite electrode materials will provide a promising research direction for the exploration of high quality supercapacitor electrode materials. It's worth noting that the specific capacitance of PEDOT:PSS/GQDs composites is higher than that of NFC/PEDOT-PSS composites. This systematic study is of great significance to the exploration of supercapacitor materials.

Electrochemical impedance spectroscopy (EIS) probes the electrical double layer effects at the electrode/electrolyte interface.[36] The PEDOT:PSS/GQDs film with compositions of 20 wt.% GQDs and PEDOT:PSS were compared by EIS to understand their electrochemical properties. The Nyquist plots of PEDOT:PSS/GQDs composite and PEDOT:PSS was show in Fig. 2F obtained in the frequency range of 100 kHz to 0.05 Hz and is characteristic of capacitive type behavior. In the high frequency domain (inset), the intercept of the plot with the real axis represents solution resistance ( $R_s$ ), a same negligible  $R_s$  for the two film is observed, which means that the increase in GQDs did not affect the hydrophilicity of the electrode and they have a same fast ion diffusion ability.[37] The size of the semicircle is determined by the charge transfer resistance ( $R_{ct}$ ) at the interface between the electrode material and the electrolyte, which were determined from the diameters of the semicircles. The  $R_{ct}$  values of PEDOT:PSS and PEDOT:PSS/GQDs increased 20 wt.% GQDs are arranged as follows,  $7.5 \Omega$  (PEDOT:PSS) <  $12.5 \Omega$  (PEDOT:PSS/GQDs), a larger interfacial resistance for the film implying that the ion in the electrolyte has difficulty to penetrate the electrode material that may due to a Faradaic reaction that involves the exchange of  $H^+$  between the electrolyte and electrode.[37] The gap between them is small, the smaller semicircle showed good electrode contact, which indicated a good connection between the electrode and electrolyte. In the low-frequency part of the plot, both curves tend to be vertical line, implying that the supercapacitors show almost ideal capacitive behavior, representing good ion diffusion in the electrode structure.

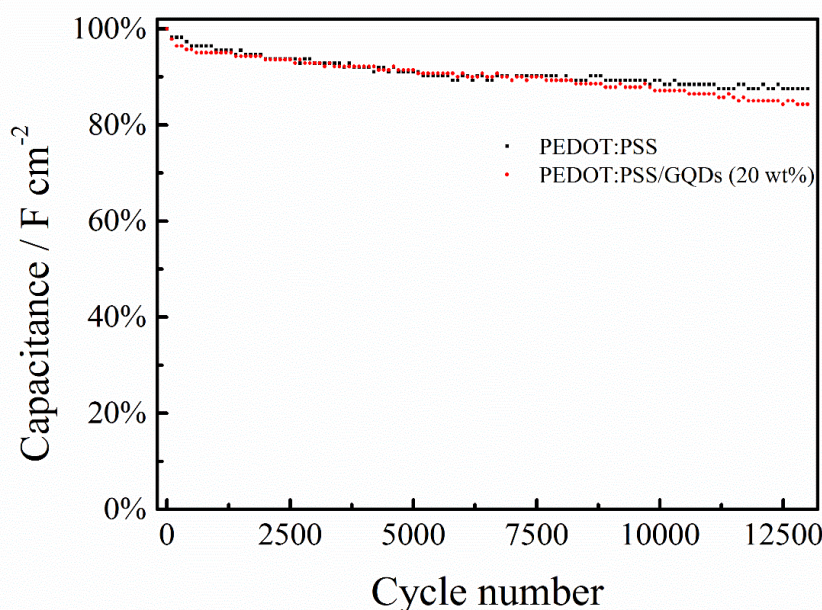


**Figure 3.** Cycling stability of PEDOT:PSS and PEDOT:PSS/GQDs film with varying GQDs concentrations at a current density  $1 \text{ Ag}^{-1}$  in  $1 \text{ M H}_2\text{SO}_4$  electrolyte system, showing the long-term cycling stability.

Ultra-long cycling stability is one of the important indexes to measure the performance of supercapacitors, and excellent stability is the necessary guarantee for the service life of supercapacitors equipment.[38] Here, ultra-long cycling stability measurements of PEDOT:PSS/GQDs (20wt.%) and PEDOT:PSS film were conducted for 13,500 cycles in air condition as show in Fig.3. From the analysis of long-term stability curves, both of them have better long-term stability, that is, the PEDOT:PSS/GQDs composite film displayed excellent capacity retention well over 84% of the initial value over 13500 consecutive charging/discharging cycles compared to the reported nanostructured composites based PEDOT:PSS[39, 40] and the stability of PEDOT:PSS/GQDs is a little weaker than that of pure PEDOT:PSS (87%).

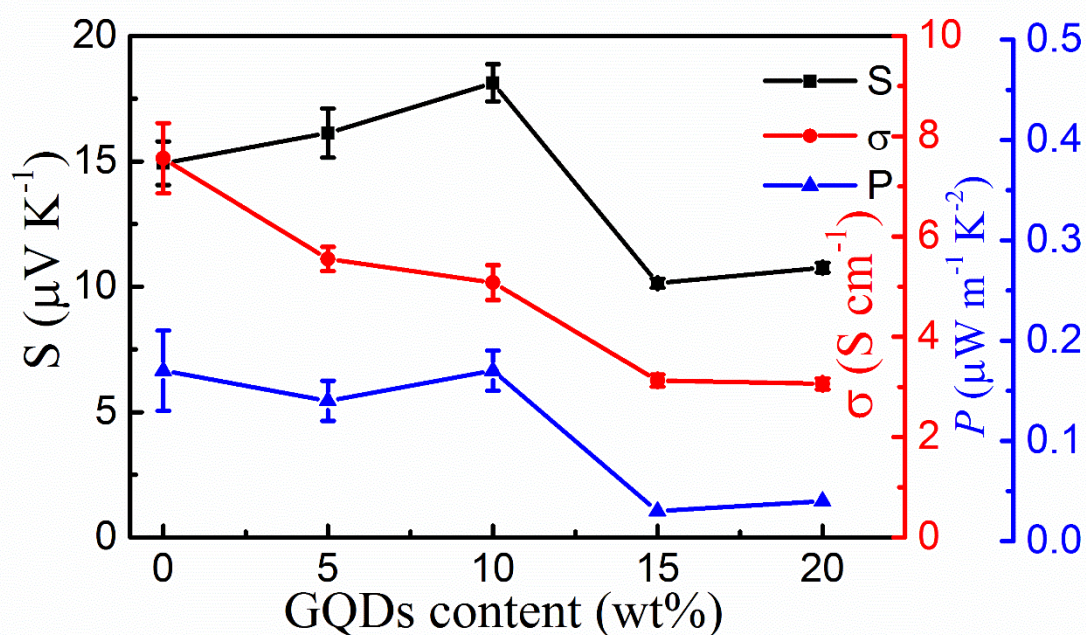


**Figure 4.** Electrical conductivity, Seebeck coefficient and power factor of PEDOT:PSS/GQDs composites film with different mass ratios GQDs.

### 3.2. Thermoelectric performance

Thermoelectric (TE) materials are important branch in the research field of novel energy storage materials, are a promising energy harvest material that can easily convert heat directly into electrical voltage through the Seebeck effect.[41] The TE performance is usually measured by the dimensionless figure of merit  $ZT$  defined by the formula,  $ZT = S^2sT/k$ , where the power factor  $PF$  ( $PF = S^2s$ ) is also an important indicator to estimate the TE performance.[42] Here, the  $S$  and  $s$  values of the composite films containing different mass ratios were obtained by Keithley 2700 and 2401 systems and conventional four-probe technique, as shown in Fig. 4. From the curve analysis, it can be concluded that

the conductivity of the PEDOT:PSS/GQDs composite film decreases regularly with the concentration range of 10 wt.% GQDs. The trade-off relationship between  $s$  and  $S$  of TE materials is well known and at the same time obtained the optimum PF value ( $3.3 \text{ mW m}^{-1} \text{ K}^{-2}$ ). The significant improvements are attributed to the orderly arrangement of PEDOT chains on the GQDs surface,[43] which stems from the strong interfacial interaction between PEDOT:PSS and GQDs and the separation of PEDOT and PSS phases. This systematic study on the thermoelectric properties of PEDOT:PSS/GQDs composite will provide important reference value for the search for novel high-performance thermoelectric materials.

#### 4. CONCLUSION

In the present work, we have prepared PEDOT:PSS/GQDs films containing variable GQDs components by vacuum filtration method. The as-prepared films were then tested for the electrochemical performance of the three-electrode system to explore their capacitive performance. CV curves of PEDOT:PSS/GQDs with different contents of GQDs films show enhanced capacitance and typical pseudocapacitance behavior in 0.1 M aqueous sulfuric acid electrolyte solution in the potential range from -0.2 to 0.8 V. As compared to the PEDOT:PSS film, the specific capacitance increases with the increase of GQDs concentration calculated by the constant current charge-discharge curve and reaches its maximum value at 20 w% and the film has good reversibility and rate capability. In addition, the PEDOT:PSS/GQDs with 20 w% GQDs concentration displays excellent capacity retention well over 84% of the initial value over 13500 consecutive charging/discharging cycles. All the capacitance behaviors results indicate that the as-prepared PEDOT:PSS/GQDs film has improved capacitive performance which is due to the addition of suitable amount of GQDs, which is attributed to its unique properties such as large specific surface area, abundant active sites and accessible edges. Here it is expected that the composite containing of PEDOT:PSS and GQDs components with good capacitive performance will provide more possibilities for the preparation of novel electrodes for supercapacitor applications.

#### ACKNOWLEDGEMENTS

This work was supported by the financial support of National Natural Science Foundation of China (11564015), the Jiangxi Provincial Department of Education (GJJ190584, GJJ190612, and GJJ180631) and the Special Foundation for Outstanding Young Talents of Jiangxi Science and Technology Normal University (2015QNBjrc002).

#### References

1. Y. Zhu, N. Li, T. Lv, Y. Yao, H. Peng, J. Shi, S. Cao and T. Chen, *J. Mater. Chem. A*, 6 (2018) 941.
2. C. Zhao, X. Jia, K. Shu, C. Yu, G. G. Wallace and C. Wang, *J. Mater. Chem. A*, 8 (2020) 4677.
3. L. Fu, Q. Qu, R. Holzea, V. V. Kondratiev and Y. Wu, *J. Mater. Chem. A*, 7 (2019) 14937.
4. J. Zhang, S. Seyedin, S. Qin, P. A. Lynch, Z. Wang, W. Yang, X. Wang and Joselito M. Razal, *J. Mater. Chem. A*, 7 (2019) 6401.

5. W. Yan, J. Li, G. Zhang, L. Wang and D. Ho, *J. Mater. Chem. A*, 8 (2020) 554.
6. J. Edberg, O. Inganäs, I. Engquist and M. Berggren, *J. Mater. Chem. A*, 6 (2018) 145.
7. M. M. Islam, C. M. Subramaniyam, T. Akhter, S. N. Faisal, A. I. Minett, H. K. Liu, K. Konstantinov and S. X. Dou, *J. Mater. Chem. A*, 5 (2017) 5290.
8. S. Khasim, A. Pasha, N. Badi, M. Lakshmi and Y. K. Mishra, *RSC Adv.*, 10 (2020) 10526.
9. F. Wang, X. Wu, X. Yuan, Z. Liu, Y. Zhang, L. Fu, Y. Zhu, Q. Zhou, Y. Wu and W. Huang, *Chem. Soc. Rev.*, 46 (2017) 6816.
10. J. Wu, Z. Lan, J. Lin, M. Huang, Y. Huang, L. Fan, G. Luo, Y. Lin, Y. Xie and Y. Wei, *Chem. Soc. Rev.*, 46 (2017) 5975.
11. M. Zhi, C. Xiang, J. Li, M. Li and N. Wu, *Nanoscale*, 5 (2013) 72.
12. R. Wang, M. Han, Q. Zhao, Z. Ren, X. Guo, C. Xu, N. Hu and L. Lu, *Sci. Rep.*, 7 (2017) 44562.
13. Y. Huang, H. Li, Z. Wang, M. Zhu, Z. Pei, Q. Xue, Y. Huang and C. Zhi, *Nano Energy*, 22 (2016) 422.
14. S. Sahoo and J.-J. Shim, *J. Ind. Eng. Chem.*, 54 (2017) 205.
15. S. Shivakumara and N. Munichandraiah, *J. Alloys Compd.*, 787 (2019) 1044.
16. D. Zhao, Q. Zhang, W. Chen, X. Yi, S. Liu, Q. Wang, Y. Liu, J. Li, X. Li and H. Yu, *ACS Appl. Mater. Interfaces*, 9 (2017) 13213.
17. H. U. Lee, J. L. Yin, S. W. Park and J. Y. Park, *Synth. Met.*, 228 (2017) 84-90.
18. C. Yin, H. Zhou and J. Li, *Ionics*, 25 (2018) 685.
19. R. J. da Silva, R. M. A. P. Lima, M. C. A. de Oliveira, J. J. Alcaraz-Espinoza, C. P. de Melo and H. P. de Oliveira, *J. Electroanal. Chem.*, 856 (2020) 113658.
20. Z. Su, C. Yang, C. Xu, H. Wu, Z. Zhang, T. Liu, C. Zhang, Q. Yang, B. Li and F. Kang, *J. Mater. Chem. A*, 1 (2013) 12432.
21. T. Cheng, Y.-Z. Zhang, J.-P. Yi, L. Yang, J.-D. Zhang, W.-Y. Lai and W. Huang, *J. Mater. Chem. A*, 4 (2016) 13754.
22. G. Cai, P. Darmawan, M. Cui, J. Wang, J. Chen, S. Magdassi and P. S. Lee, *Adv. Energy Mater.*, 6 (2016) 1501882.
23. X. Jian, H.-m. Yang, J.-g. Li, E.-h. Zhang, L.-l. Cao and Z.-h. Liang, *Electrochim. Acta*, 228 (2017) 483.
24. Y. Niu, J. Wang, J. Zhang and Z. Shi, *J. Electroanal. Chem.*, 282 (2018) 1.
25. S. N. J. S. Z. Abidin, M. S. Mamat, S. A. Rasyid and Y. Sulaiman, *Electrochim. Acta*, 261 (2018) 548.
26. Q. Chen, Y. Hu, C. Hu, H. Cheng, Z. Zhang, H. Shao and L. Qu, *Phys. Chem. Chem. Phys.*, 16 (2015) 19307.
27. Y. Liu, R. Wang, J. Lang and X. Yan, *Phys. Chem. Chem. Phys.*, 17 (2015) 14028.
28. W.-W. Liu, Y.-Q. Feng, X.-B. Yan, J.-T. Chen and Q.-J. Xue, *Adv. Funct. Mater.*, 23 (2013) 4111.
29. W. Zhang, Y. Yang, R. Xia, Y. Li, J. Zhao, L. Lin, J. Cao, Q. Wang, Y. Liu and H. Guo, *Carbon*, 162 (2020) 114.
30. W. Liu, M. Zhang, M. Li, B. Li, W. Zhang, G. Li, M. Xiao, J. Zhu, A. Yu and Z. Chen, *Adv. Energy Mater.* 10 (2020) 1903724.
31. I. K. Moon, B. Ki and J. Oh, *Chem. Eng. J.*, 392 (2020) 123794.
32. C. Sun, X. Li, J. Zhao, Z. Cai and F. Ge, *Electrochim. Acta*, 317 (2019) 42.
33. A. K. Cuentas Gallegos and M. E. Rincón, *J. Power Sources*, 162 (2006) 743-747.
34. D. Antiohos, G. Folkes, P. Sherrell, S. Ashraf, G. G. Wallace, P. Aitchison, A. T. Harris, J. Chen and A. I. Minett, *J. Mater. Chem.*, 21 (2006) 15987.
35. M. M. Islam, A. T. Chidembo, S. H. Aboutaleb, D. Cardillo, H. K. Liu, K. Konstantinov and S. X. Dou, *Front. Energy Res.*, 2 (2014).
36. T. Cheng, Y.-Z. Zhang, J.-D. Zhang, W.-Y. Lai and W. Huang, *J. Mater. Chem. A*, 4 (2016) 10493-

10499.

37. N. Kumar, R. T. Ginting and J.-W. Kang, *Electrochim. Acta*, 270 (2018) 37-47.
38. S. Su, L. Lai, R. Wang, L. Zhang, Y. Cui, R. Li, N. Guo, W. Shi and X. Zhu, *J. Alloys Compd.*, 834 (2020) 154477.
39. M. N. Dang, T. H. Nguyen, T. V. Nguyen, T. V. Thu, H. Le, M. Akabori, N. Ito, H. Y. Nguyen, T. L. Le, T. H. Nguyen, V. T. Nguyen and N. H. Phan, *Nanotechnology*, 31 (2020) 345401.
40. F. González, P. Tiemblo and M. Hoyos, *Appl. Sci.* 9 (2019) 3371.
41. Y. Ma, W. Yuan, Y. Bai, H. Wu and L. Cheng, *Carbon*, 154 (2019) 292.
42. R. Tjandra, W. Liu, M. Zhang and A. Yu, *J. Power Sources*, 438 (2019) 227009.
43. A. T. Lawal, *Biosensors & bioelectronics*, 141 (2019) 111384.
44. S. N. J. S. Z. Abidin, M. S. Mamat, S. A. Rasyid and Z. Zainal, *Electrochim. Acta*, 261 (2017) 548.
45. S. H. Kazemi and S. Abdollahi Aghdam, *J. Electron. Mater.*, 48 (2019) 5088.
46. D. Antiohos, G. Folkes, P. Sherrell, S. Ashraf, G. G. Wallace, P. Aitchison, A. T. Harris, J. Chen and A. I. Minett, *J. Mater. Chem.*, 21 (2011) 15987.
47. D. S. Patil, S. A. Pawar and J. C. Shin, *J. Ind. Eng. Chem.*, 62 (2018) 166.
48. S. Fratini, M. Nikolka, A. Salleo, G. Schweicher and H. Sirringhaus, *Nat. Mater.*, 19 (2020) 491.
49. F. Zhang and C.-a. Di, *Chem. Mater.*, 32 (2020) 2688.
50. F. P. Du, N. N. Cao, Y. F. Zhang, P. Fu, Y. G. Wu, Z. D. Lin, R. Shi, A. Amini and C. Cheng, *Sci. Rep.*, 8 (2018) 6441.

© 2020 The Authors. Published by ESG ([www.electrochemsci.org](http://www.electrochemsci.org)). This article is an open access article distributed under the terms and conditions of the Creative Commons Attribution license (<http://creativecommons.org/licenses/by/4.0/>).